Supplementary information

Synthesis of Water-Soluble Gold-Aryl Nanoparticles with Distinct Catalytic Performance in the Reduction of the Environmental Pollutant 4-Nitrophenol

Ahmad A. L. Ahmad,[a] Seema Panicker,[b] Mohamed M. Chehimi,[c] Miguel Monge,[d] Jose M. Lopez-de-Luzuriaga,[d] Ahmed A. Mohamed,*[b] Alice E. Bruce*[a] and Mitchell R. M. Bruce*[a]

[a] *Department of Chemistry, University of Maine, Orono, ME 04469, USA*

[b] *Center for Advanced Materials Research, Research Institute for Science and Engineering, University of Sharjah, Sharjah 27272, UAE*

[c] *Institut de Chimie et des Matériaux Paris Est (ICMPE)-SPC-UMR 7182 CNRS-Université Paris Est Créteil, 2-8 rue Henri Dunant, 94320 Thiais, France*

[d] *Departamento de Química, Centro de Investigación en Síntesis Química (CISQ), Universidad de La Rioja, Complejo Científico-Tecnológico, 26006–Logroño, Spain*

List of Contents

List of Contents

Page

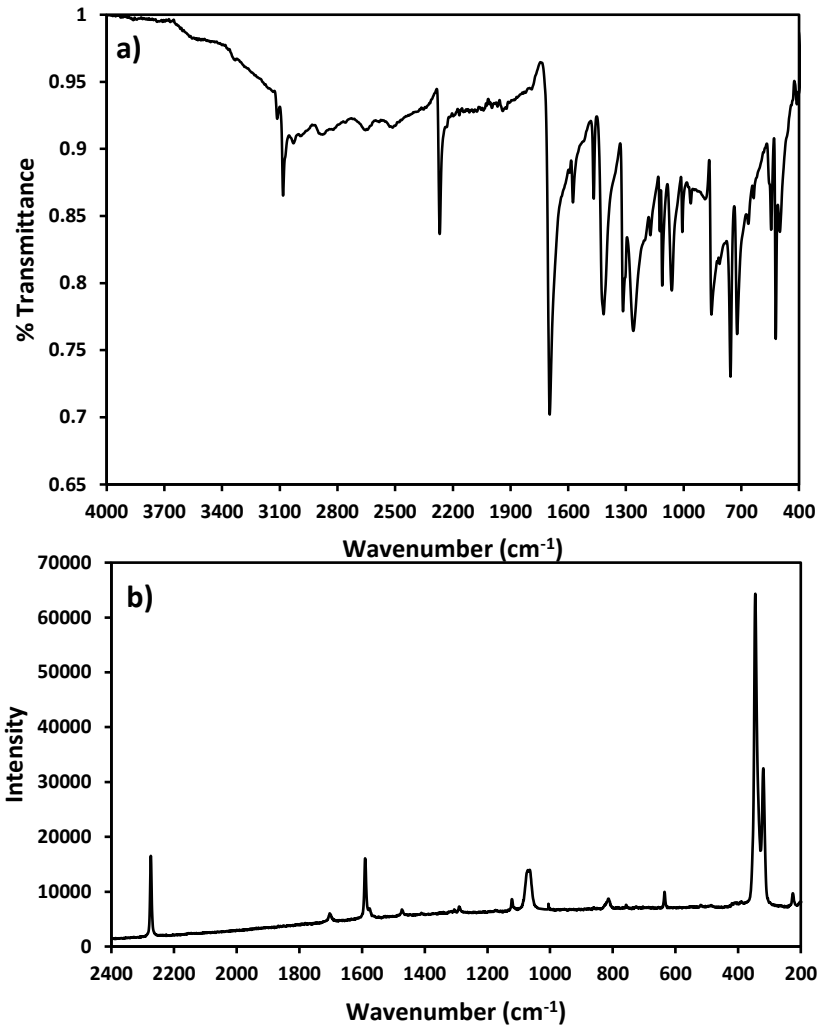

Figure S1. (a) ATR-FTIR of the diazonium gold(III) salt showing the diazonium functional peak at 2270 cm^{-1}, and (b) Raman spectrum of the aryldiazonium gold(III) salt showing the diazonium functional and the $[AuCl_4]^-$ anion peaks.

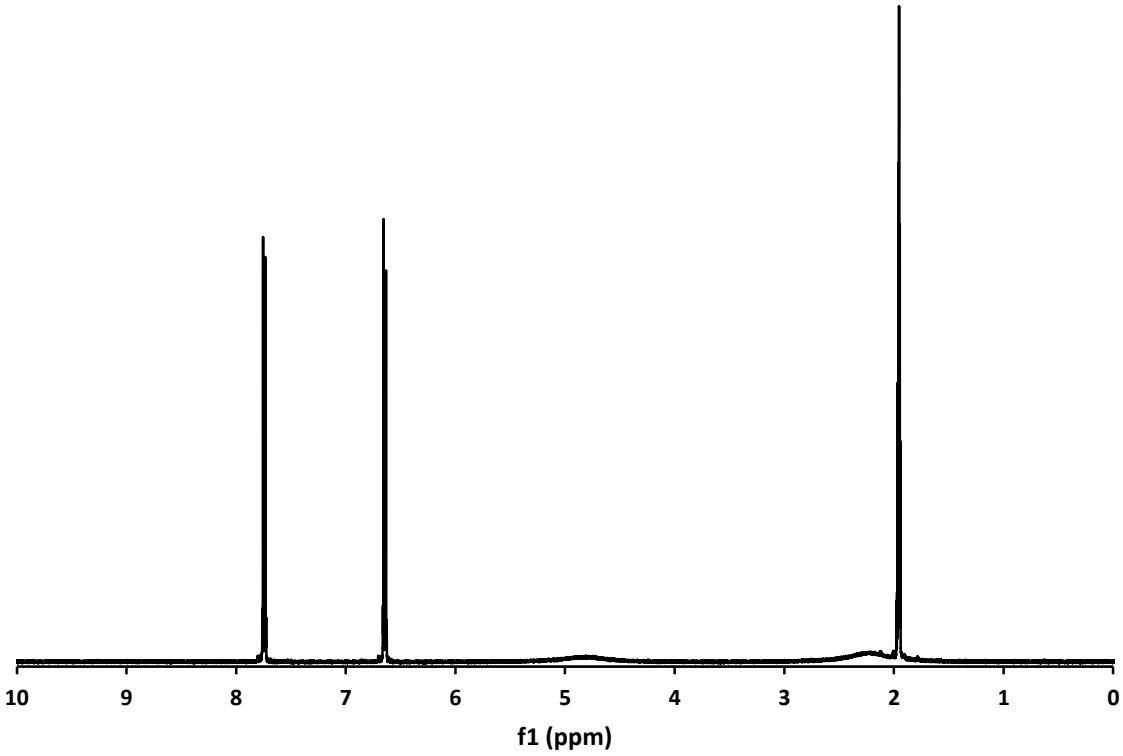

Figure S2. ^{1}H NMR spectrum of 4-aminobenzoic acid in (CD_3CN).

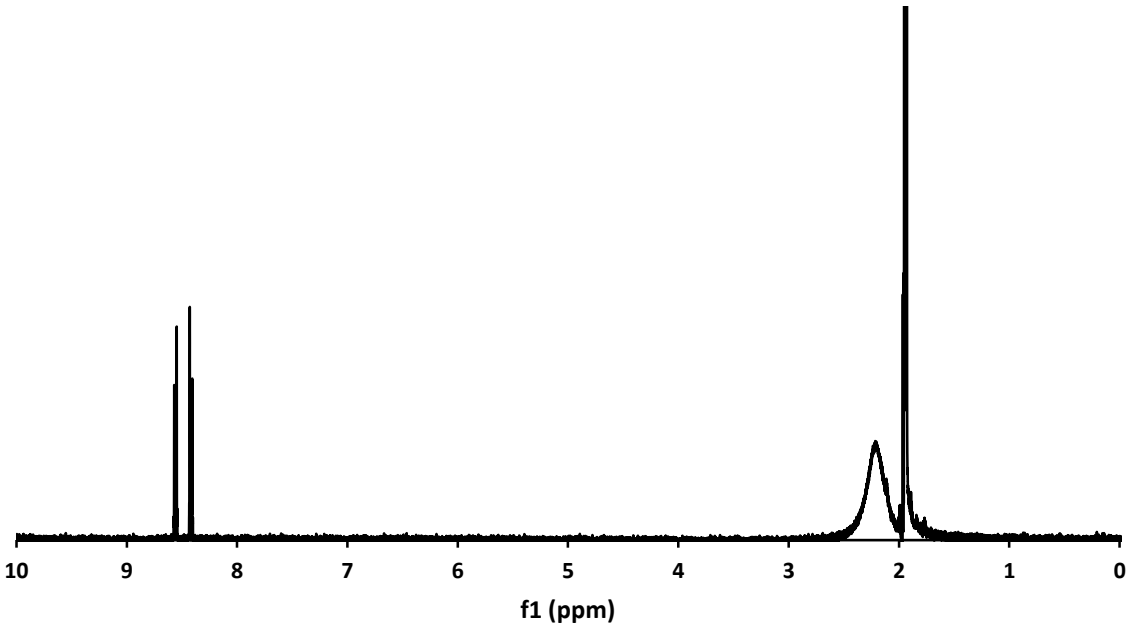

Figure S3. ^{1}H NMR spectrum of [HOOC-4-$C_6H_4N{\equiv}N$]$AuCl_4$ in (CD_3CN).

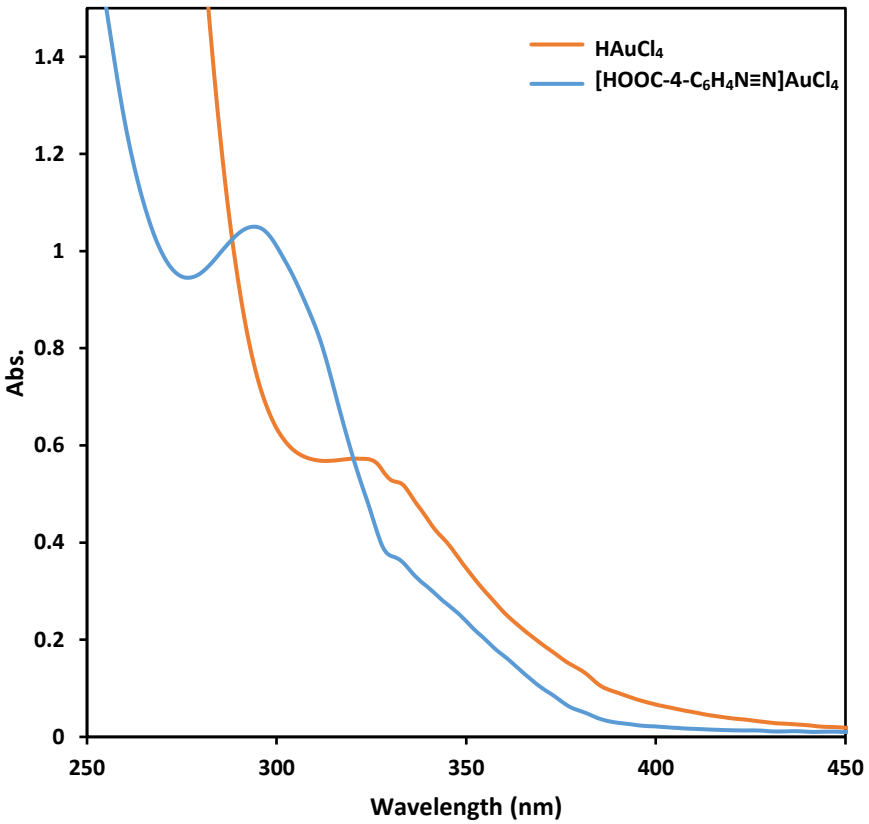

Figure S4. UV-Vis spectrum for hydrogen tetrachloroaurate(III) (0.246 M), and [HOOC-4-$C_6H_4N{\equiv}N$]$AuCl_4$ (0.123M) in deionized water.

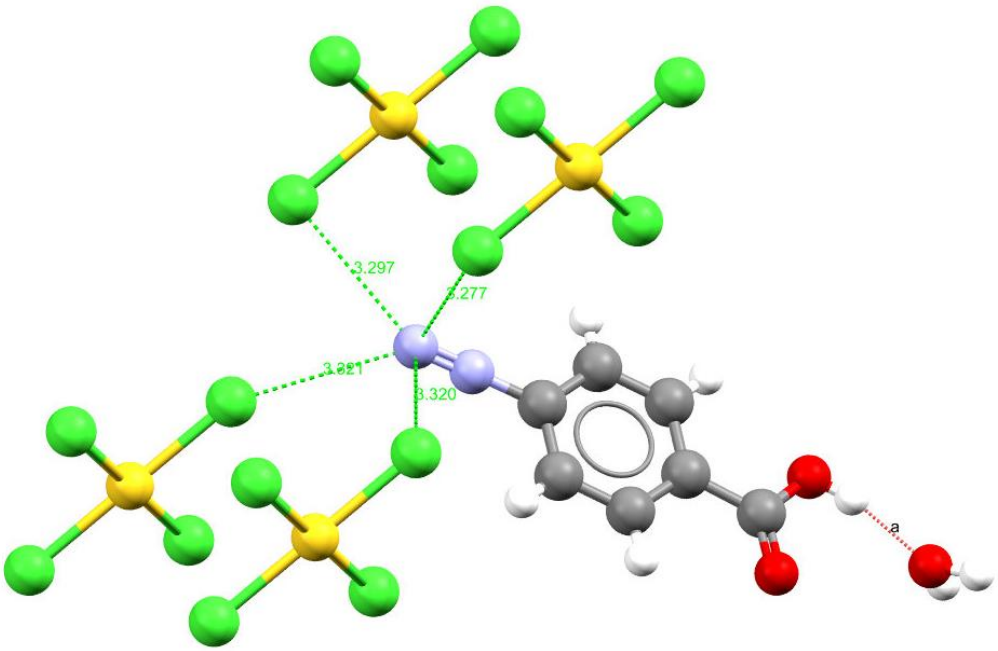

Figure S5. Model molecular structure of [COOH-4-$C_6H_4N{\equiv}N$]$AuCl_4$ showing the close proximity of the tetrachloroaurate ion to the diazonium functional.

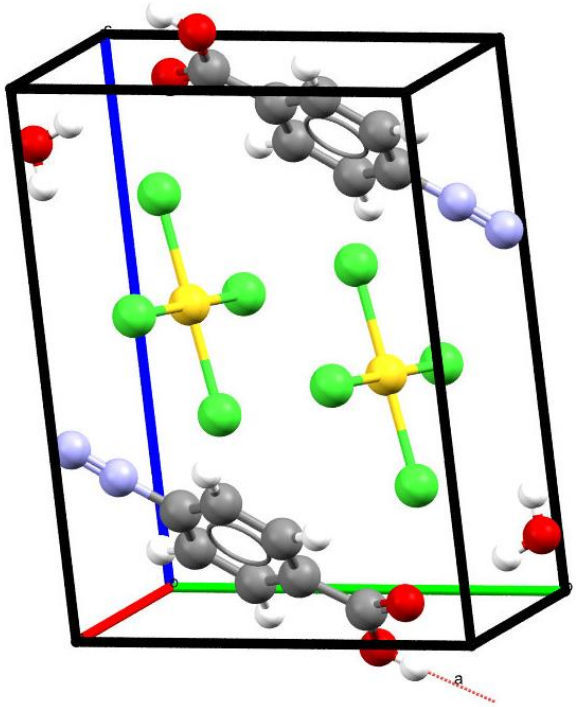

Figure S6. Packing model of [COOH-4-$C_6H_4N{\equiv}N$]$AuCl_4$ in the unit cell.

Table S1. Crystal data and structure refinement for [COOH-4-$C_6H_4N{\equiv}N$]$AuCl_4$.

Empirical formula	$C_7H_5AuCl_4N_2O_2.H_2O$
Formula weight (g/mole)	505.92
Temperature (K)	296.15
Crystal system	Triclinic
Space group	P-1
a (Å)	7.831(2)
b (Å)	7.931(2)
c (Å)	11.079(3)
α (˚)	97.173(15)
β (˚)	95.533(15)
γ (˚)	96.097(15)
Volume ($Å^3$)	674.7(3)
Z	2
ρ_{calc} (g/cm^3)	2.490
μ (mm^{-1})	11.690
F(000)	465.9
Crystal size/mm^3	0.249 × 0.213 × 0.127
Radiation	Mo Kα (λ = 0.71073)
2Θ range for data collection/°	5.214 to 50.048
Index ranges	$-9 \leq h \leq 9$, $-9 \leq k \leq 9$, $-13 \leq l \leq 13$
Reflections collected	6474
Independent reflections	2370 [R_{int} = 0.0776, R_{sigma} = 0.0936]
Data/restraints/parameters	2370/3/152
Goodness-of-fit on F^2	1.012
Final R indexes [I>=2σ (I)]	R_1 = 0.0445, wR_2 = 0.0838
Final R indexes [all data]	R_1 = 0.0770, wR_2 = 0.0937
Largest diff. peak/hole / e $Å^{-3}$	1.35/-2.00

Table S2. Bond distances (Å) and angles (˚) for [COOH-4-$C_6H_4N{\equiv}N$]$AuCl_4$.

Bond distances (Å)			
Au1-Cl1	2.275(3)	C1-C2	1.3900
Au1-Cl2	2.270(3)	C1-C6	1.3900
Au1-Cl3	2.285(3)	C2-C3	1.3900
Au1-Cl4	2.272(3)	C3-C4	1.3900
O1-C7	1.195(13)	C4-C7	1.470(12)
N2-N1	1.079(12)	C4-C5	1.3900
O2-C7	1.317(12)	C6-C5	1.3900
N1-C1	1.347(11)		

Bond angles (˚)			
Cl2-Au1-Cl1	179.74(12)	C3-C2-C1	120.0
Cl3Au1-Cl1	89.88(12)	C4-C3-C2	120.0
Cl3-Au1-Cl2	90.16(11)	C7-C4-C3	116.5(6)
Cl4-Au1-Cl1	90.13(12)	C5-C4-C3	120.0
Cl4-Au1-Cl2	89.83(11)	C5-C4-C7	123.5(6)
Cl4-Au1-Cl3	179.86(14)	O2-C7-O1	123.78(10)
C1-N1-N2	177.1(13)	C4-C7-O1	112.9(10)
C2-C1-N1	119.6(6)	C4-C7-O2	123.3(10)
C6-C1-N1	120.4(6)	C5-C6-C1	120.0
C6-C1-C2	120.0	C6-C5-C4	120.0

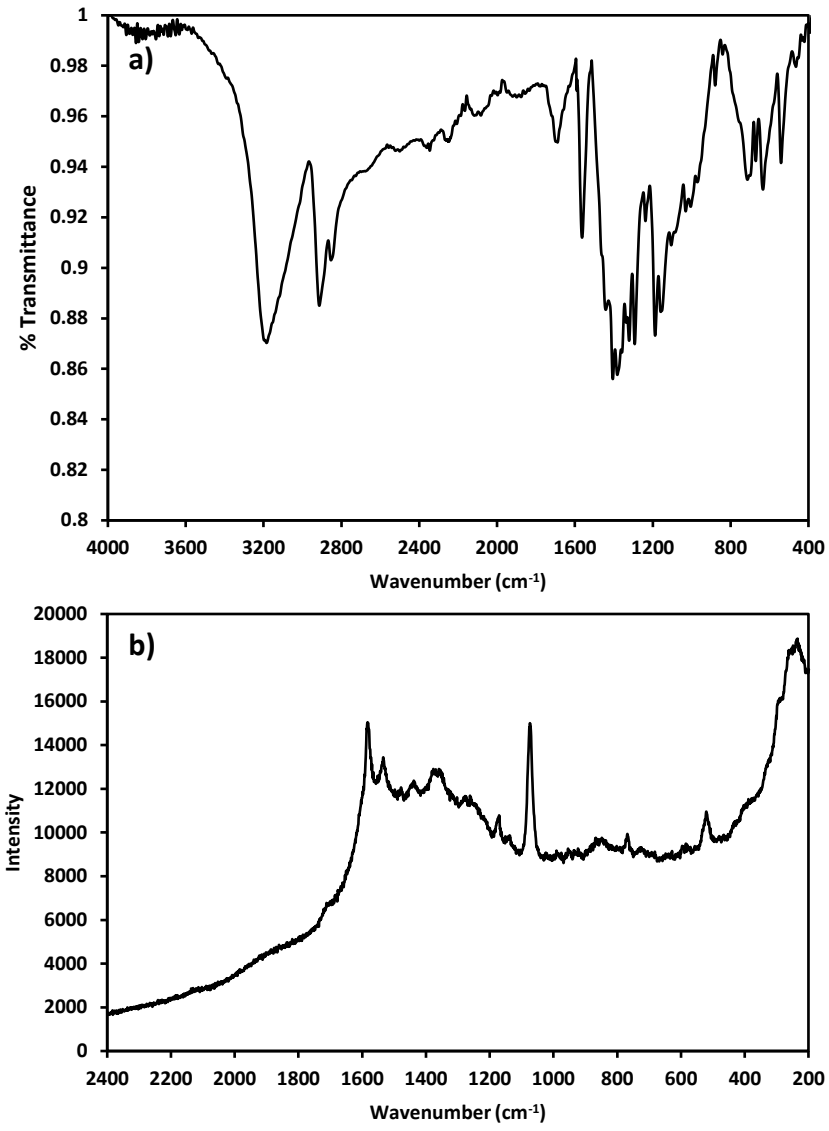

Figure S7. (a) ATR-FTIR spectrum of AuNPs-COOH, and (b) Raman spectrum of AuNPs-COOH, showing the absence of diazonium functional peak.

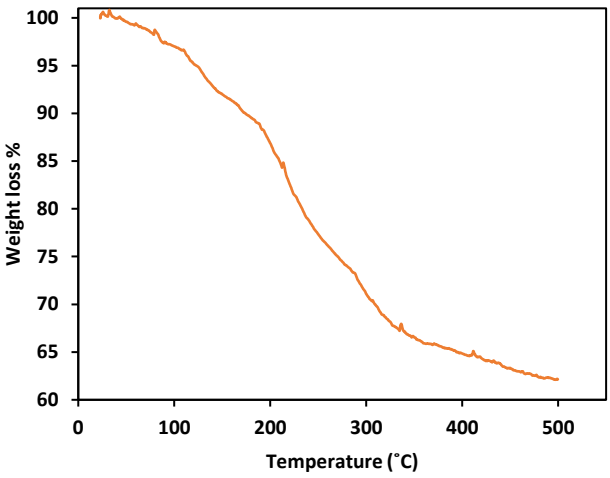

Figure S8. TGA measurement of the AuNPs-COOH nanoparticles.

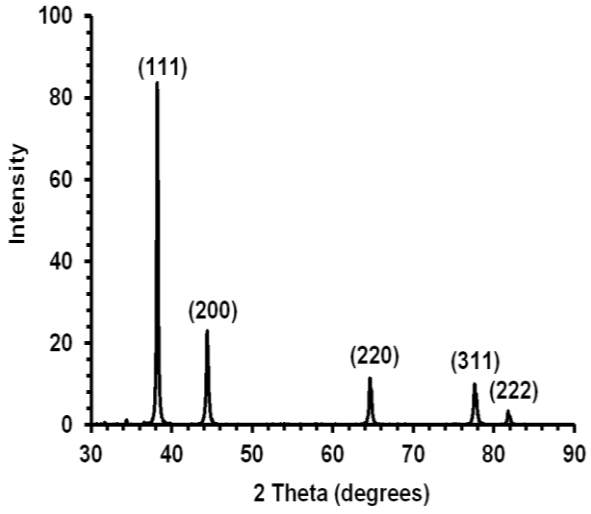

Figure S9. XRD analysis of AuNPs-COOH.

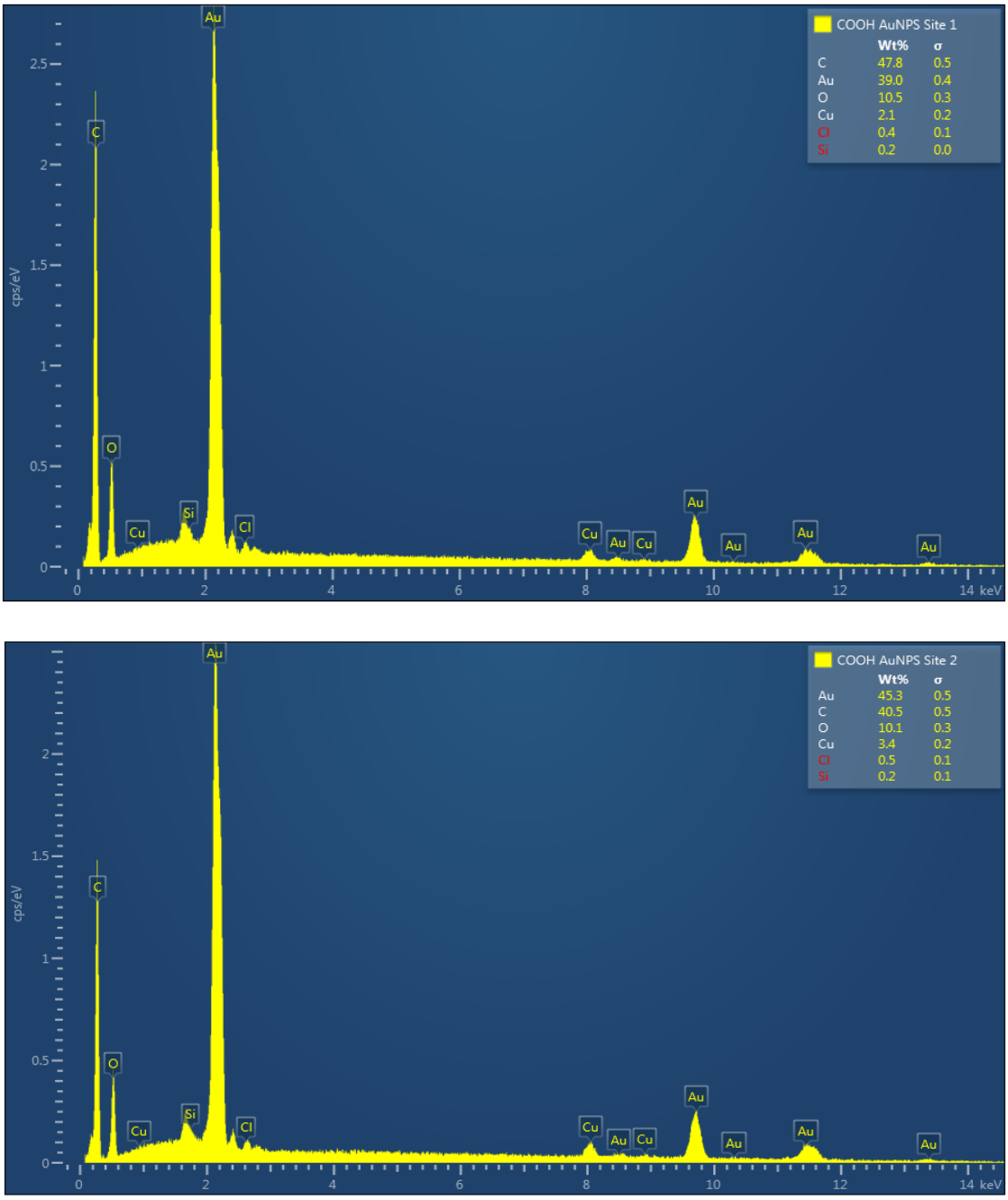

Figure S10. Two sites EDS study of AuNPs-COOH with Au= 42.2%, C= 44.2%, and O= 10.3% as average wt%.

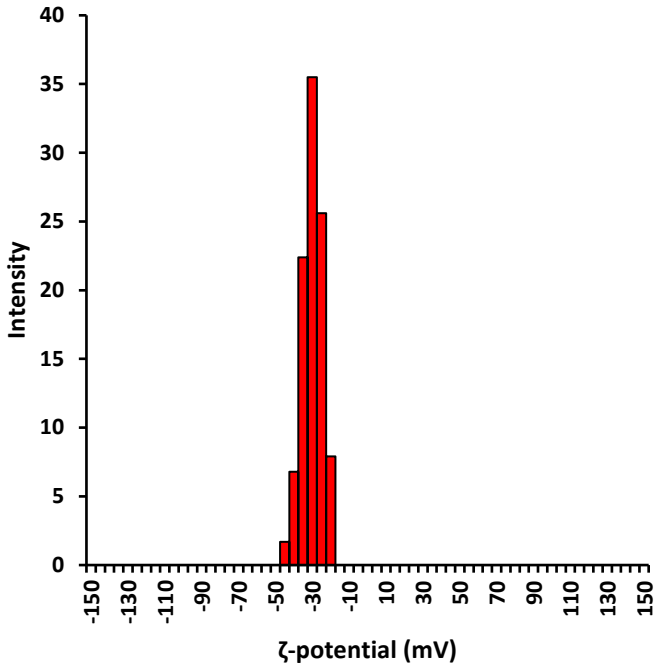

Figure S11. Average ζ-potential spectra of AuNPs-COOH dispersed in water at 25˚C.

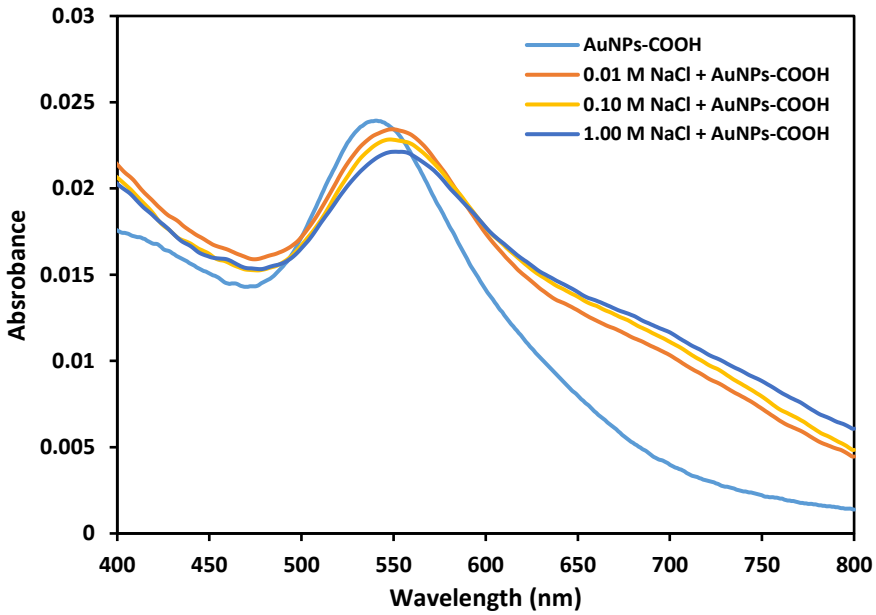

Figure S12. UV-Vis spectra of AuNPs-COOH recorded after 30 min. incubation with varying NaCl concentrations.

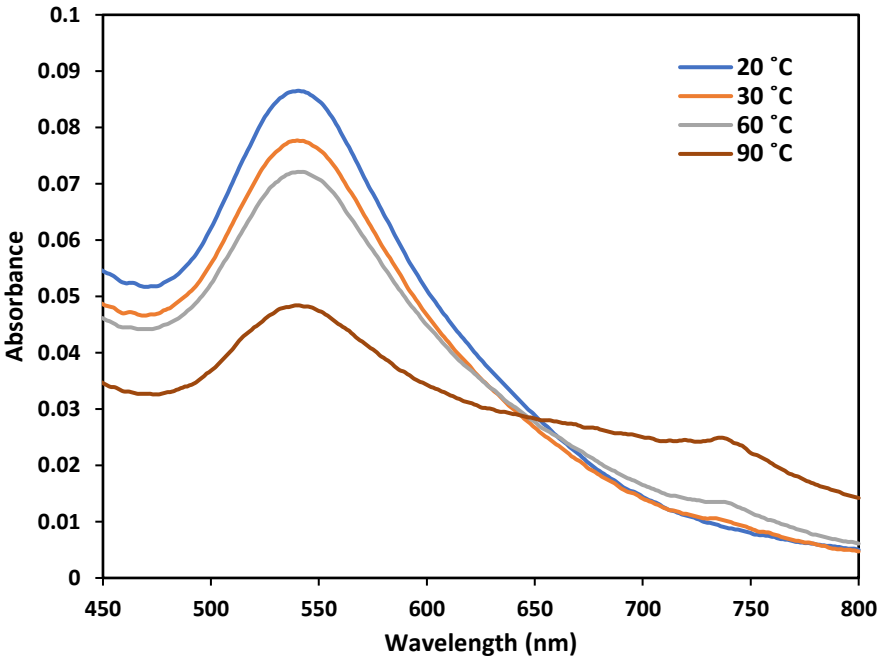

Figure S13. UV-Vis of aqueous solution of AuNPs-COOH at different temperatures.

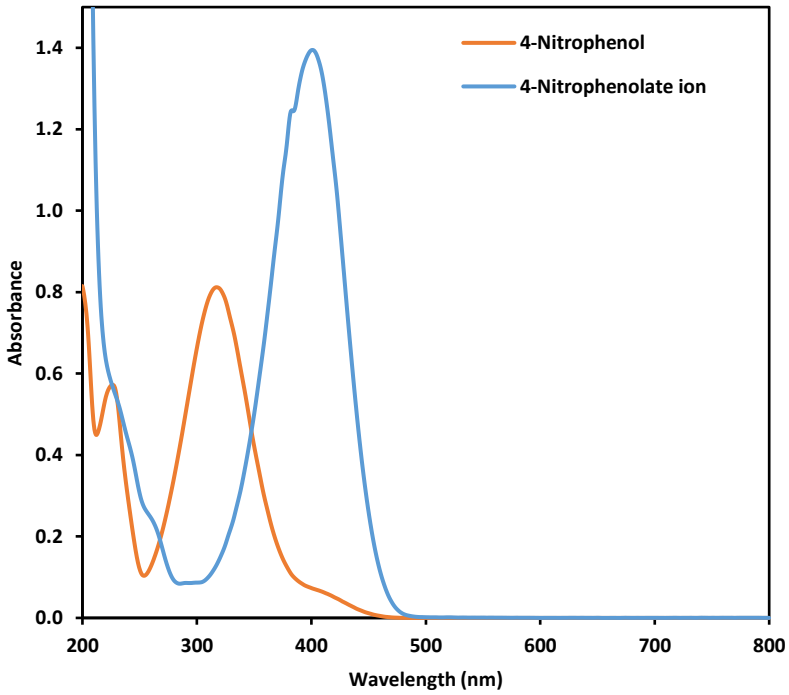

Figure S14. UV-Vis spectra of aqueous solution of 4-NPh and 4-nitrophenolate (formed upon addition of $NaBH_4$).

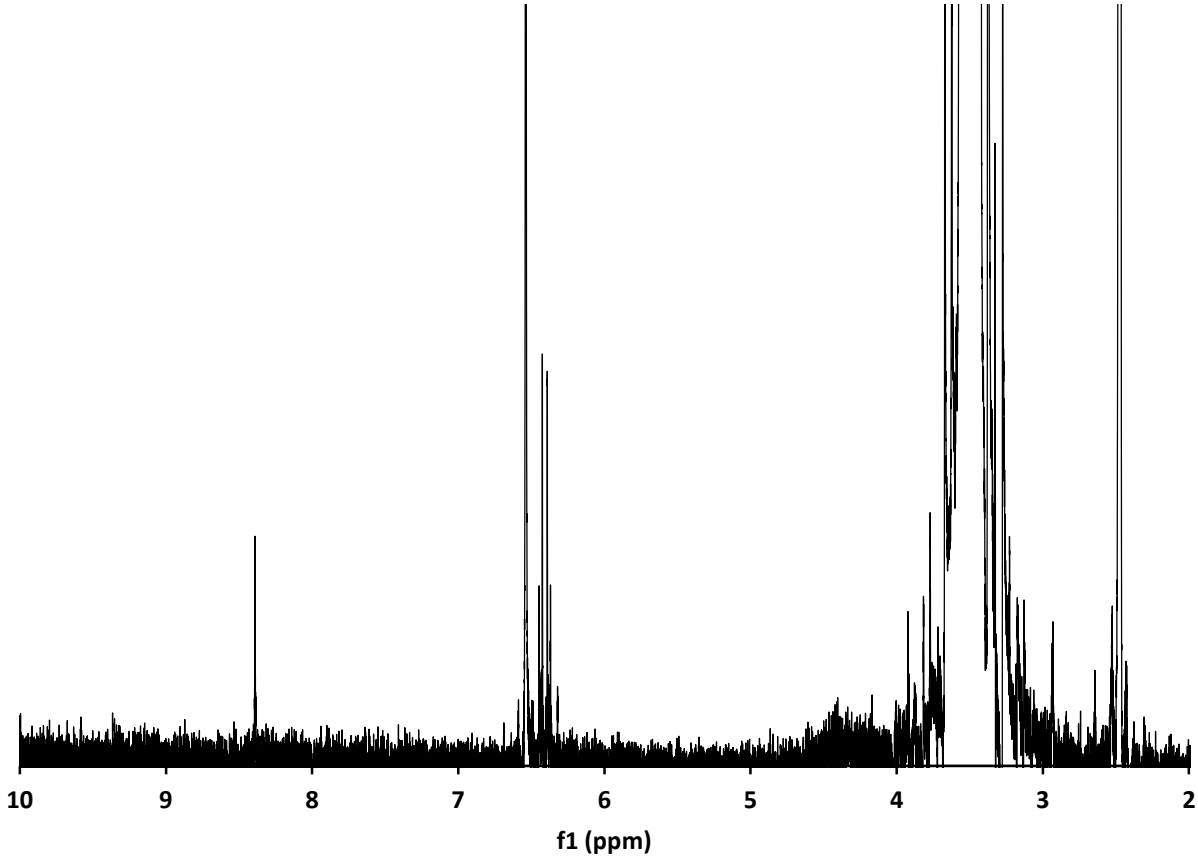

Figure S15. ^{1}H-NMR spectrum (in DMSO-d_6) of 4-APh extracted from reaction mixture.

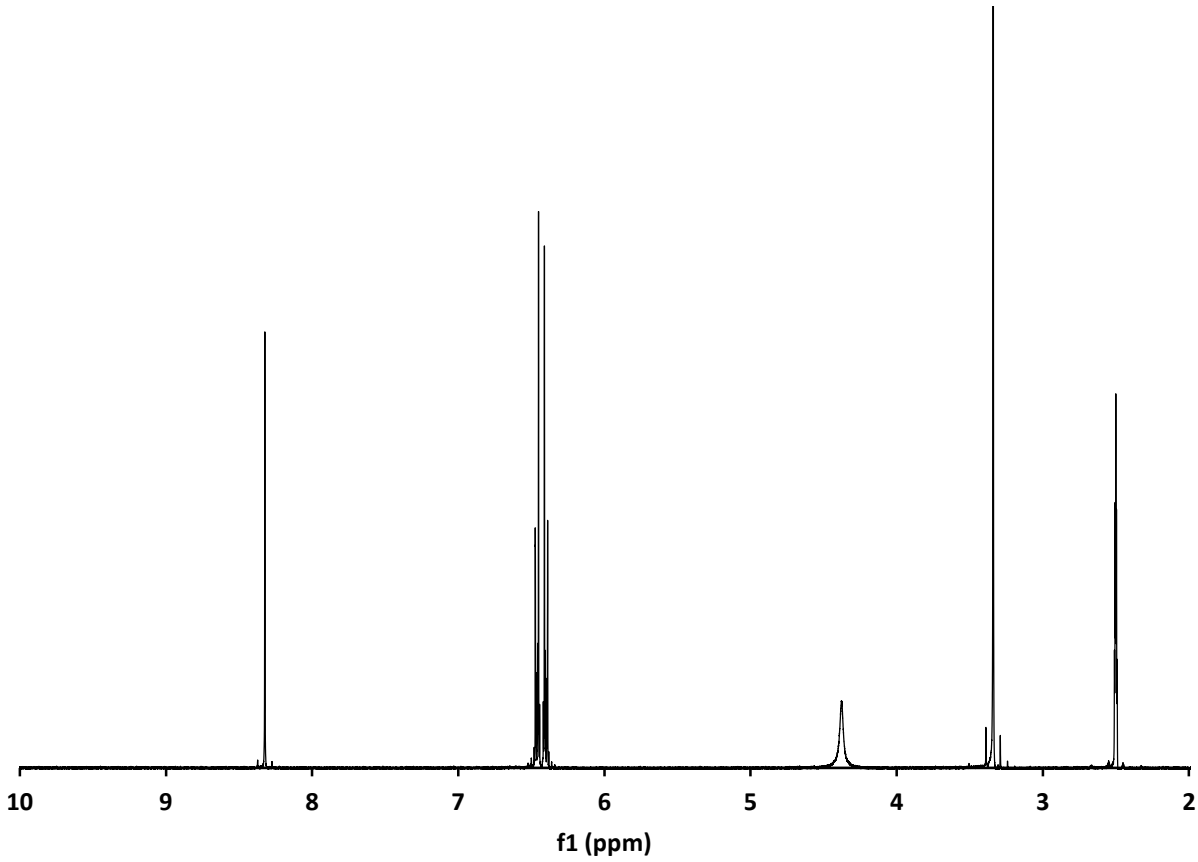

Figure S16. ^{1}H-NMR spectrum (in DMSO-d_6) of an authentic sample of 4-APh.

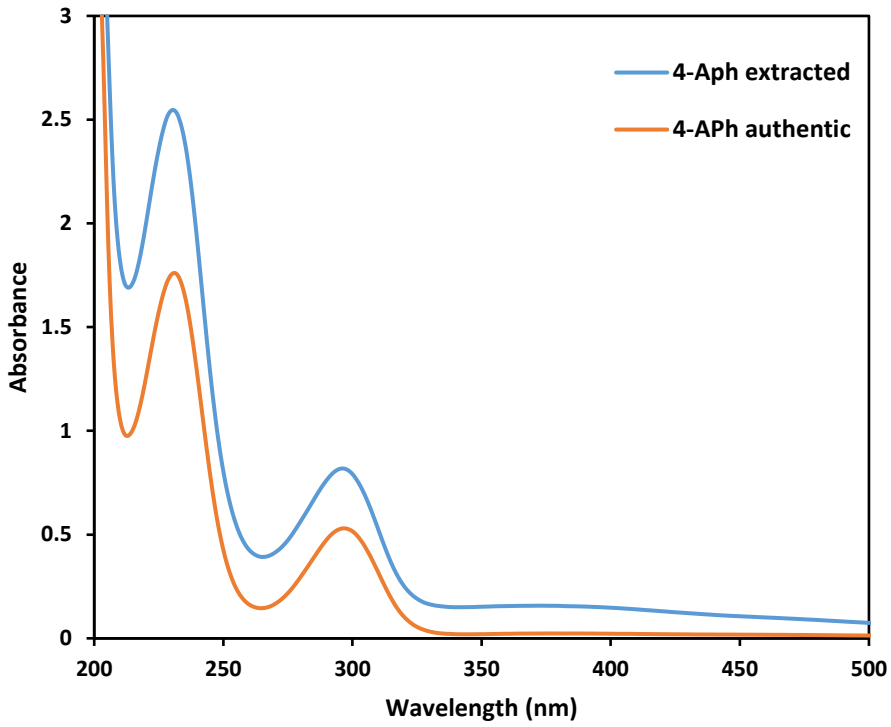

Figure S17. UV-Vis spectra of 4-APh extracted from the reduction reaction mixture and authentic 4-APh.

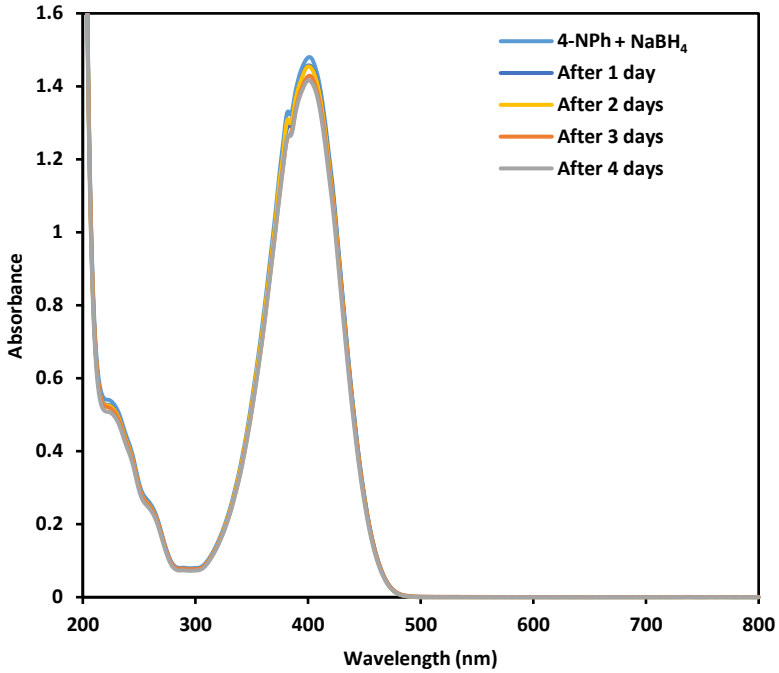

Figure S18. UV-Vis spectra of 4-NPh with $NaBH_4$ mixture in the absence of AuNPs-COOH which that no reaction even after 4 days, min ([$NaBH_4$] = 0.024 M, and [4-NPh] = 80 µM).

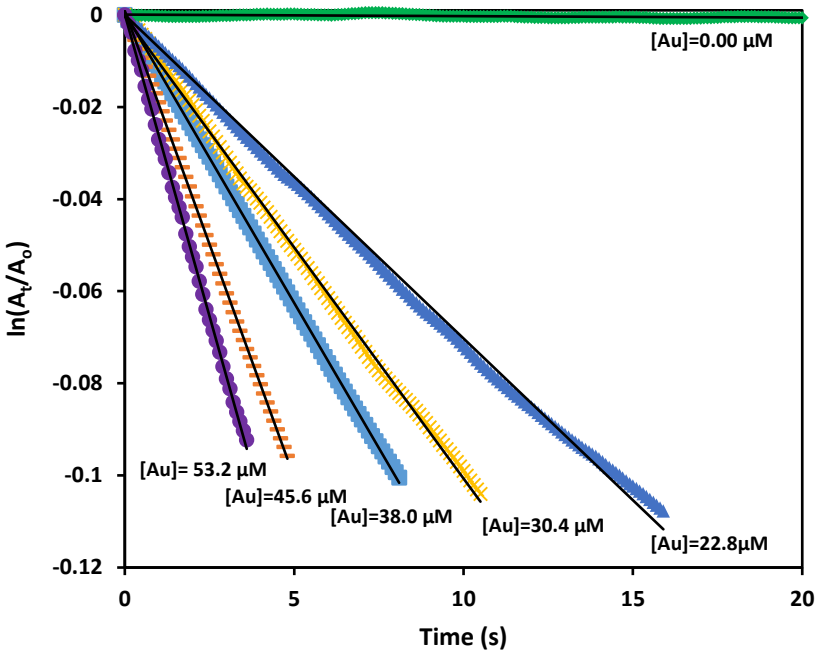

Figure S19. Plot of $\ln(A_t/A_o)$ vs. time for different concentrations of total gold. Data were taken from the initial portion of the absorbance vs time curve following the induction time. ($[NaBH_4]$ = 0.024 M, and [4-NPh] = 80 µM).

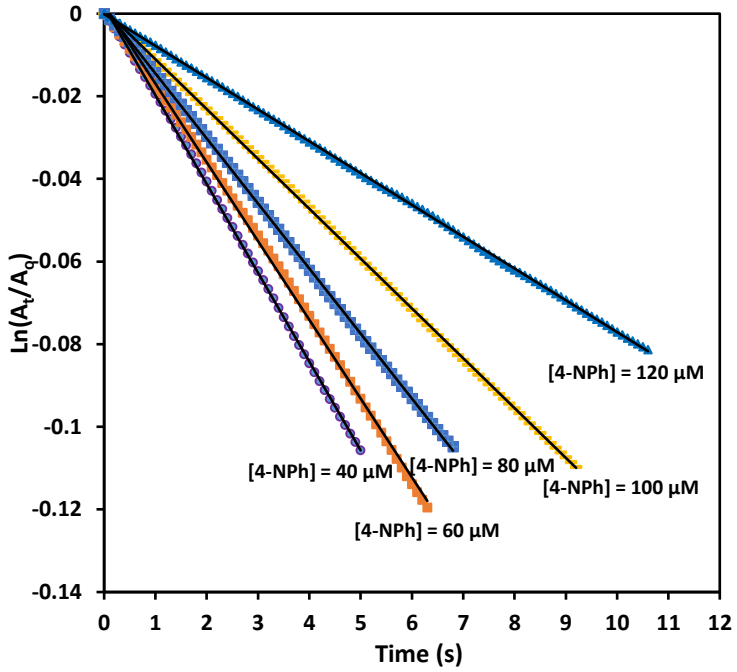

Figure S20. Plot of $\ln(A_t/A_o)$ vs. time for different concentrations of 4-NPh. Data were taken from the initial portion of the absorbance vs time curve following the induction time. ($[NaBH_4]$ = 0.024 M, and [Au] = 38 µM).

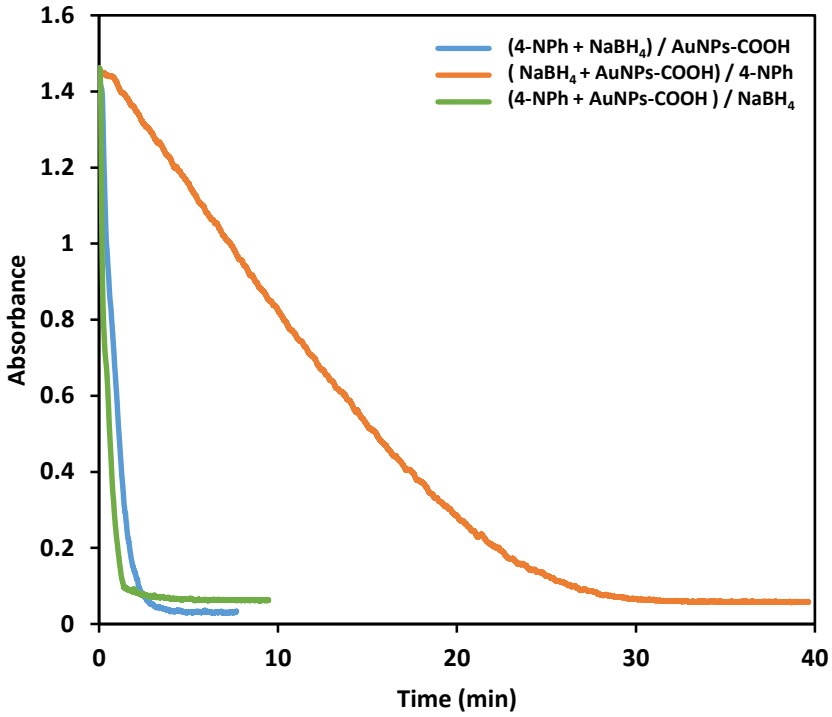

Figure S21. Reduction of 4-NPh catalyzed by AuNPs-COOH with different reactant addition sequences. The first two components enclosed in parenthesis in the figure legend were incubated for 5 min prior to addition of the third component. Monitoring of the reaction began immediately upon addition of the 3rd component by measuring the absorbance vs time for the 4-NPh peak at 400 nm; [$NaBH_4$] = 0.024 M, [4-NPh] = 80 µM, and [Au]= 38.0 µM.

Table S3. Induction time and k_{app} for reduction of 4-NPh catalyzed by AuNPs-COOH with different reactant addition sequences.

Components addition order	**Induction time (s)**	**k_{app} (s^{-1})**
(4-NPh + AuNPs-COOH) / $NaBH_4$	12.2 ± 1.4	0.108 ± 0.014
(4-NPh + $NaBH_4$) / AuNPs-COOH	19.8 ± 1.5	0.041 ± 0.006
(AuNPs-COOH + $NaBH_4$) / 4-NPh	67.6 ± 7.8	0.002 ± 0.009

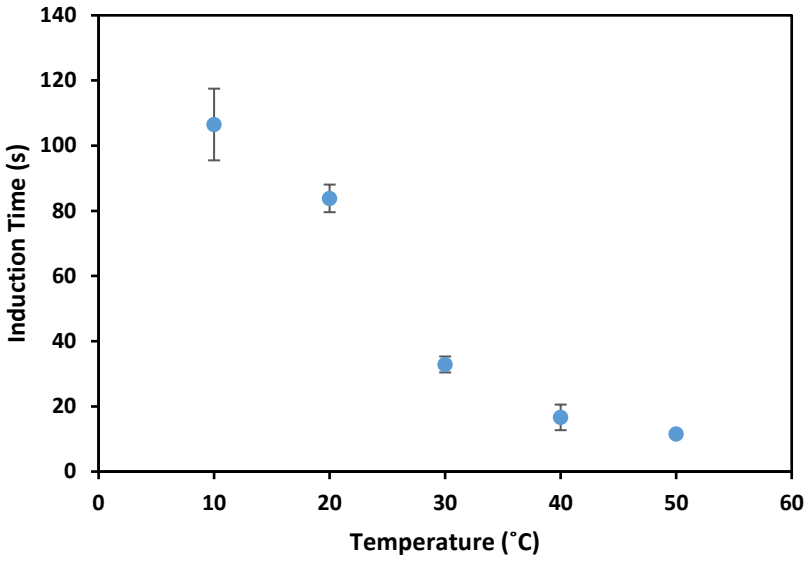

Figure S22. Induction time for reduction of 4-NPh reaction at different temperatures; [$NaBH_4$] = 0.024 M, [4-NPh] = 80 µM, and [Au]= 38.0 µM; error bars are one standard deviation of 3 trials.

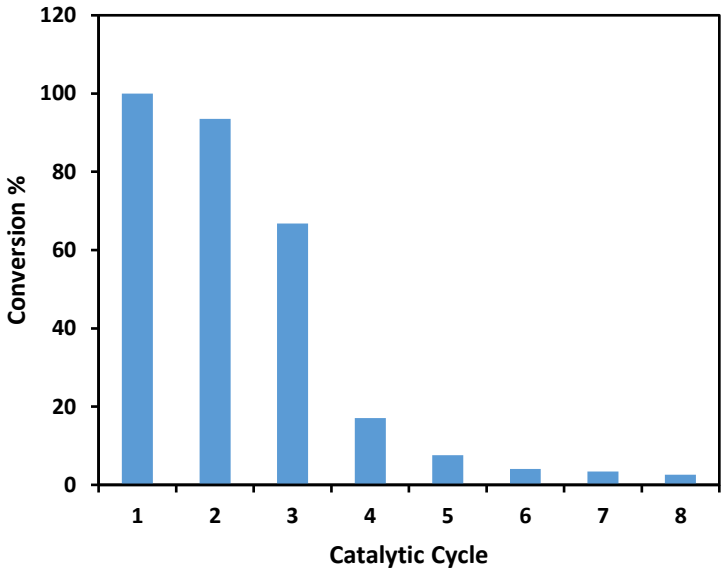

Figure S23. Comparison of 4-NPh percent conversion between eight reduction cycles after 5 mins from the beginning of the reaction cycle.

Table S4. k_{app} and time needed to complete the 4-NPh reduction reaction with $NaBH_4$ using AuNPs-COOH as a catalyst.

Cycle	k_{app} (x 10^{-2} s^{-1})	Time needed to complete the reduction reaction (min)
1	1.58	5.2
2	1.05	9.7
3	0.71	11.0
4	0.22	15.1
5	0.16	18.2
6	0.12	28.6
7	0.08	39.5
8	0.05	59.4

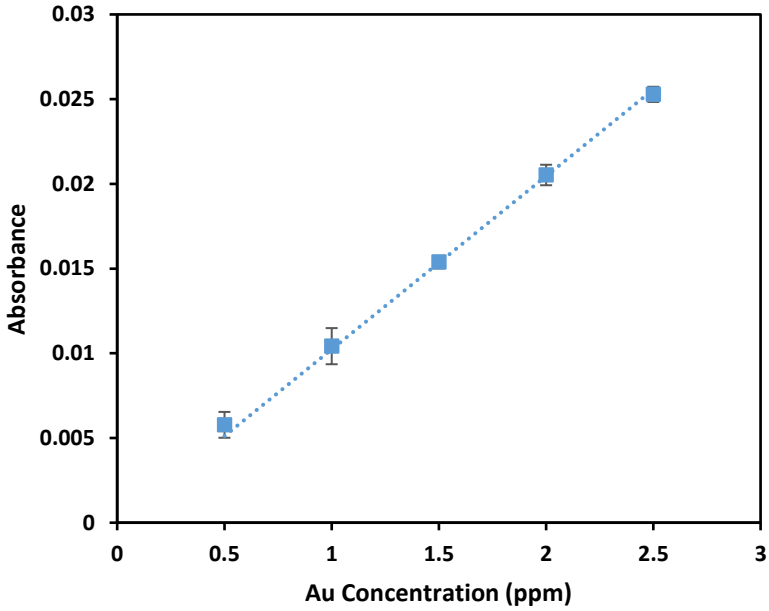

Figure S24. Calibration curve from the atomic absorption spectroscopy for the AuNPs-COOH used to calculate the concentration of gold in the nanoparticles; error bars are one standard deviation of 3 trials.